15TH IEA HEAT PUMP CONFERENCE
MAY 26–29, 2026 | HOFBURG
VIENNA 2026
DECARBONISATION THROUGH INNOVATION

Development of High-Efficiency Centrifugal Heat Pump using HFO-1233zd(E) with global warming potential of 1

Yuki Shimizu[a], Kazuma Fukasawa[a], Tomonori Nitta[a], Miki Kaneko[a], Ryosuke Suemitsu[a], Naoya Miyoshi[a], Noriyuki Matsukura[a], Kenji Ueda[a]

[a]Mitsubishi Heavy Industries Thermal Systems, Ltd., 1-1-1 Wadasaki-cho, Hyogo-ku, Kobe, Hyogo 652-8585, Japan

Abstract

We have developed a large-capacity centrifugal heat pump using HFO-1233zd(E) refrigerant with a very low (1.0) global warming potential, a low operating pressure, and a large specific volume. The compressor and heat exchanger were designed to suit these features. The heat pump provides a maximum thermal capacity of 670 kW and supplies hot-water up to 90°C using heat-source water up to 40°C. The stability and performance of the heat pump was evaluated in 90°C hot-water supply tests. Hot water at this temperature is required in the production lines of food and semiconductor factories. The results demonstrate the effectiveness of alternative refrigerants in heat pumps, which are demanded for CO_2 reduction.

Keywords: Low global warming potential refrigerant, HFO-1233zd(E), Heat pump;

1. Introduction

Production lines at various facilities, such as food and semiconductor factories, require hot water for cleaning. The hot water is often produced by boilers using energy from fossil fuels. However, the drive toward CO_2 emissions reduction and energy conservation has increased the demand for heat pumps that effectively use waste heat; moreover, this demand is growing.

Authorities worldwide have promoted regulations on refrigerants for global warming prevention. The Kigali Amendment to the Montreal Protocol, adopted in October 2016, includes a schedule for the gradual reduction of production and consumption of HFC refrigerants was determined [1]. The global warming potential (GWP) of HFC-134a, a widely used fuel in heat pumps, is 1,430, necessitating a switch to a lower-GWP refrigerant.

To this end, we developed a large-capacity centrifugal heat pump using HFO-1233zd(E) refrigerant with a GWP of 1, a low operating pressure, and a large specific volume. The compressor and heat exchanger are designed to meet these characteristics. When manufactured, the heat pump operated stably under a hot-water output condition of 90°C. The heat pump was evaluated by comparing the operational data with estimated values.

2. Heat pump design

2.1. Refrigerant Selection

Table 1 compares the performance parameters of HFC-134a and HFO refrigerants. HFO-1233zd(E) has been classified as A1 (nonflammable, lowly toxic) by the American Society of Heating, Refrigerating and Air-Conditioning Engineers (ASHRAE) and is excellently safe and available. This fuel is often used in centrifugal chillers. Fig. 1 compares the pressure–enthalpy diagrams of HFC-134a at an evaporation temperature of 7°C and a condensation temperature of 37°C with those of HFO-1233zd(E) and HFC-134a at an evaporation temperature of 30°C and a condensation temperature of 90°C. When supplied to a hot water 90°C heat pump, HFO-1233zd(E) allows a much lower condenser pressure than HFC-134a, and the pressure band approaches the case of HFC-134a in air conditioning applications. Therefore, the design pressure of the heat pump can be reduced and the wall thicknesses of the different parts (compressor, heat exchanger, and piping) can be set equal to those of a centrifugal chiller supplied with HFC-134a. Moreover, as HFO-1233zd(E) has a high theoretical coefficient of performance (COP), it is expected to improve the performance of the heat pump.

Table 1. Comparison of refrigerants

Refrigerant	HFC-134a	HFO-1234yf	HFO-1234ze(E)	HFO-1233zd(E)
Global warming potential (GWP)	1,430 *1	＜1 *2	＜1 *2	1 *2
Safety Class *2	A1	A2L	A2L	A1
Saturation pressure [MPa.G] (at 90°C) *3	3.143	2.979	2.374	0.732
Saturated gas density [kg/m^3] (at 90°C) *3	216.8	269.1	160.6	44.4
Theoretical COP [-] *4	2.799	2.366	2.797	3.341

*1 IPCC Fourth Assessment Report.[2] *1 IPCC fifth Assessment Report.[3]
*2 Refrigerant Safety Classification Standard ASHRAE 34 (A1: nonflammable, lowly toxic, A2L: lowly flammable, lowly toxic)
*3 Refprop Ver10.0 refrigerant thermal property database [4]
*4 The theoretical COP is calculated at an evaporation temperature of 14°C, a condensation temperature of 82°C, a compressor efficiency of 80%, and a single-stage refrigeration cycle.

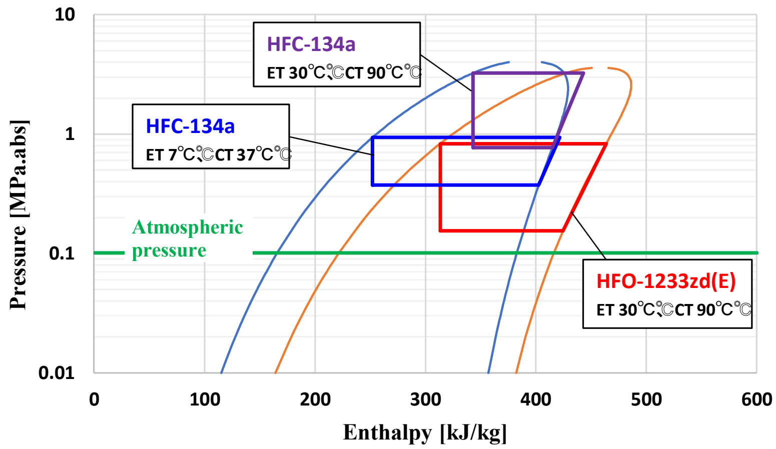

Figure 1. Comparison of pressure–enthalpy diagrams of HFC-134a and HFO-1233zd(E) [4]

2.2. Design of components

The developed heat pump uses the components of centrifugal chillers and is designed to operate over a wide range of hot-water outlet temperatures (50°C–90°C) and heat-source water outlet temperatures (5°C–35°C). High-temperature events are considered in the design of each component.

2.2.1. Compressor

The compressor is a centrifugal type with a high head and large-volume flow rate impeller shape. The compression ratio and flow rate are approximately 40% and 39% larger than those of chiller compressors, respectively, and the adiabatic efficiency is improved by approximately 3.5% from that of a chiller compressor with the same impeller diameter [5]. In addition, the rotation speed can be suppressed by using the difference in physical properties. The Mach number and rotation speed are expressed by the following equation: $M=2\pi dN/a$ (M: Mach number[-], d: Impeller diameter[m], N: Number of rotation speed[/s], a: Sound speed[m/s]). The gas sound speed of HFO-1233zd (E) is lower than that of HFC-134a. The impeller diameter is larger since gas specific volume of HFO-1233zd (E) is larger than that of HFC-134a. Therefore, under the same heat pump conditions, the maximum rotation speed of HFO-1233zd(E) is 55% that of HFC-

134a. The range of rotation speed is equivalent to that of HFC-134a used in air conditioning, and the reliability of the equipment is ensured.

2.2.2. Heat exchanger

The heat pump uses a shell and tube heat exchanger to ensure high efficiency and a large capacity output. The shell diameter and number of tubes in the condenser and evaporator were varied to optimize the shape for the expected operating range. Fig. 2 shows samples of the void-fraction analysis in the evaporator and condenser of the heat exchanger at the maximum heat load. Fluent was used for the software. The void fraction distribution in the tube bundle of the evaporator, confirmed in this analysis, was arranged to prevent local dry-out and carry-over. To optimize the performance, liquid cutting plate is added, the drainage ability in the tube bundle of the condenser was also improved.

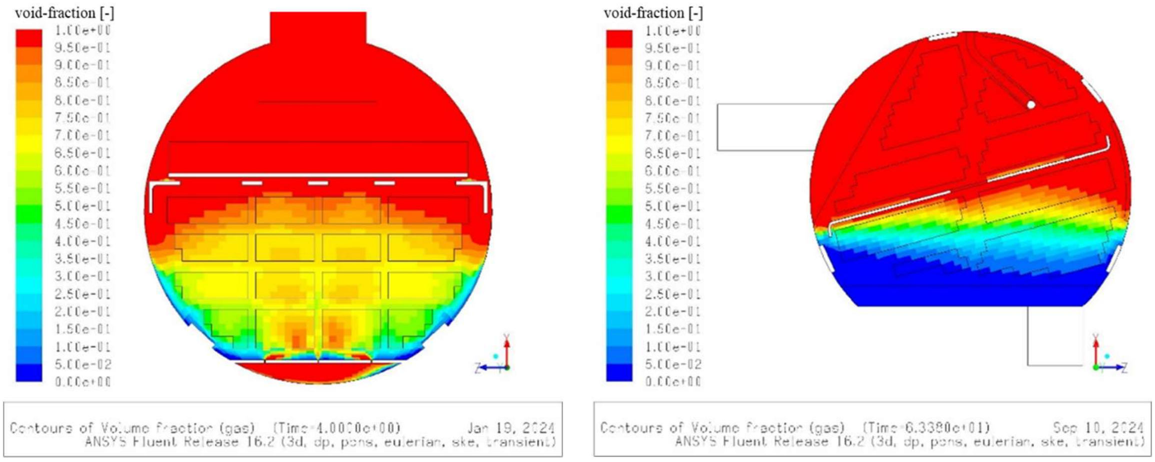

(a) Evaporator (b) Condenser

Figure 2. Example of (void fraction analysis in the) (a) evaporator and (b) condenser of the heat exchanger

When the condenser is operated at high temperature, the different coefficients of thermal expansion between the steel shell and copper tube induce thermal stress. To prevent damage to the components, the internal component structure was designed to account for the thermal stress to the stress generated by the components.

2.2.3. Oil tank

The selected lubricating oil is compatible with the refrigerant. The amount of refrigerant dissolved into lubricant oil varies with pressure. When a change in the operating conditions decreases the pressure in the oil tank, the refrigerant dissolved in the oil precipitates and foaming occurs. Owing to its large gas specific volume, HFO-1233zd(E) precipitates more gas during foaming than HFC-134a. In addition, as the heat-source water temperature is high, the evaporation pressure exceeds that of a centrifugal chiller and a large amount of the refrigerant dissolves into the lubricant oil, largely decreasing the oil viscosity. In the developed machine, the volume of the oil tank is sufficient to prevent outflow of the oil from the tank when foaming raises the oil level. The amount of gas deposition is controlled by limiting the depressurization speed of the evaporator at start-up. In addition, the oil tank is heated under the control of a heater to prevent viscosity decrease of the oil.

2.2.4. Selection of elastomer materials

Heat-resistant parts are essential because the equipment is heated to high temperature. As high heat accelerates the degradation of the elastomer materials in the valve interior and sealant, the parts were selected through an evaluation of the airtightness within the assumed operation time during continuous use with a hot water (90°C) outlet.

3. Verification test

This section verifies the unit performance of the developed heat pump. Table 2 lists the equipment specifications and Fig. 3 shows the system diagram and an external view of the verification machine. The cycle is a two-stage compression, two-stage expansion subcooled cycle. The starting method uses an inverter with a wide operating range. For compactness, the inverter unit is installed on the evaporator, and an economizer, oil tank and control panel are installed under the condenser.

Table 2. Specifications of the verification machine

Refrigerant	HFO-1233zd(E) [300kg]
Cycle	Two-stage compression, two-stage expansion subcooled cycle
Evaporator/Condenser/Sub cooler	Shell and tube type
Economizer	Tank type
External dimensions	L 3.144 m × W 1.576 m × H 1.723 m
Stating method	Inverter
Motor capacity	160 kW
Min power supply	400 V

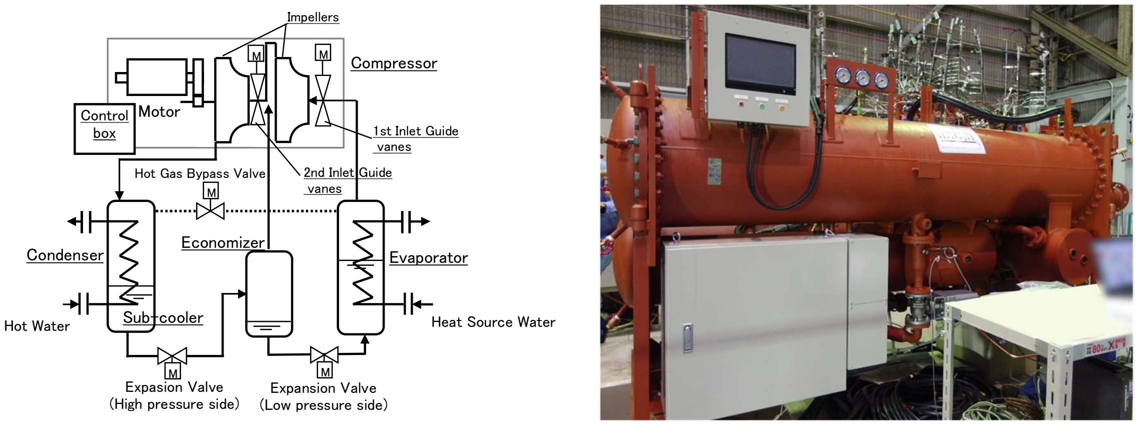

Figure 3. (left) Heat-pump cycle and (right) external view of the verification machine

Table 3 and Fig. 4 show the test results at a hot-water outlet temperature of 90°C and the data during operation, respectively. Table 3 shows 1-minute average values. The hot-water outlet temperature was stably maintained at its target value (90°C). The heating capacity exceeded 670 kW, and the heating COP almost matched the estimated value. During operation, the maximum temperature in the machine was 93.3°C at the compressor discharge. The temperature of the condenser (which approximates the condensation saturation temperature) was 90.2°C. The components selection was appropriate and the thermal stress evaluation validated, because no component damage, refrigerant leakage from joints, or air intrusion into the cabin occurred after operation.

Table 3. Operation results of the developed heat pump

		Measured value	Estimated value
Heating capacity	kW	674.7	669.7
Hot water temperature	°C	79.7 → 90.0	80.0 → 90.0
Hot water flow rate	m^3/h	58.1	59.3
Heat source water temperature	°C	40.3 → 35.1	40.0 → 35.0
Heat source water flow rate	m^3/h	85.1	87.4
Power consumption	kW	171.2	172.6
Heating COP	-	3.94	3.88
Heat balance	-	1.0012	1

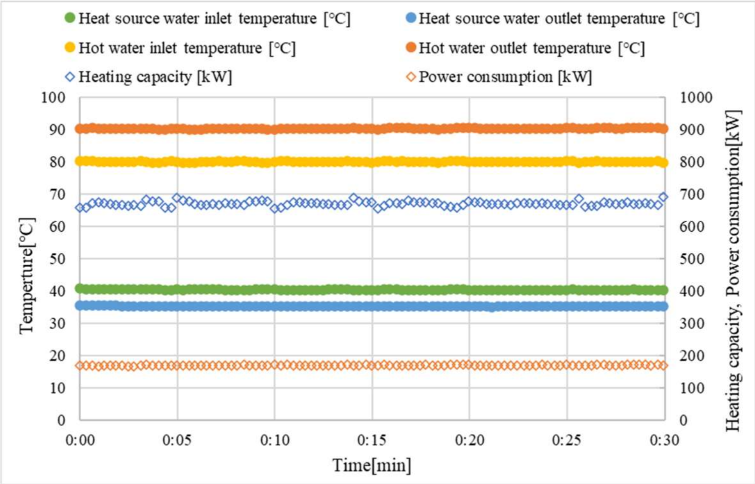

Figure 4. Operation data of the developed heat pump

Fig. 5 shows the part-load performance measurements at 80%, 60%, and 50% capacity under the conditions in Table 3. By closing the vanes, the capacity was decreased up to 60%, although the COP was maintained at approximately 4. The capacity was further lowered after opening the hot-gas bypass valve under controlled conditions. The equipment can operate at a capacity of up to 50% or lower. Fig. 6 shows the assumed operational range of the developed machine and points of actual operation. When the hot-water and heat-source water temperatures changed, the inverter rotation speed was optimally controlled according to the head, enabling wide-range operation. Therefore, the operating point of the equipment can be adjusted according to the required heating capacity and temperature in industrial applications.

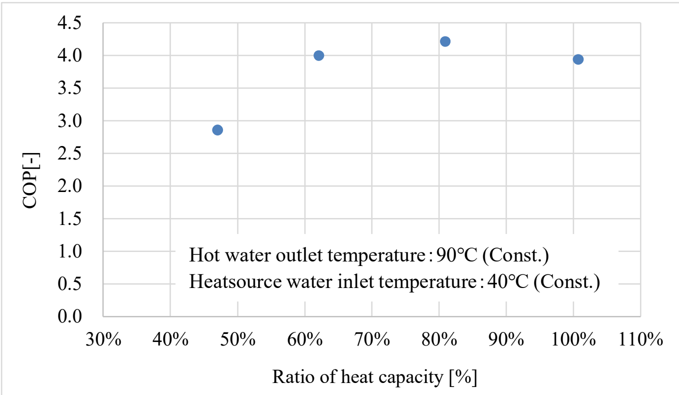

Figure 5. Part load performance of the developed heat pump

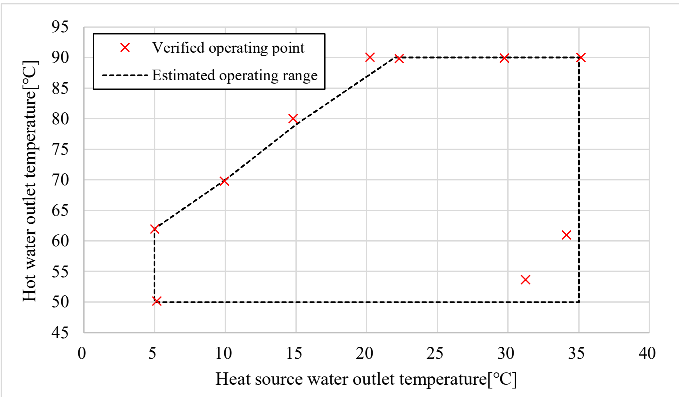

Figure 6. Operational range of the developed heat pump

4. Effect of heat pump application

The economic effect of introducing the developed heat pump was also estimated. Fig. 7 shows an example of a system with a heat pump. Fig. 8 shows the reductions in CO_2 emissions and running costs from those of a gas-fired boiler in the system shown in Fig. 7. Relative to the gas-fired boiler, the heat pump reduces the annual CO_2 emissions by 52% and the running costs by 59%.

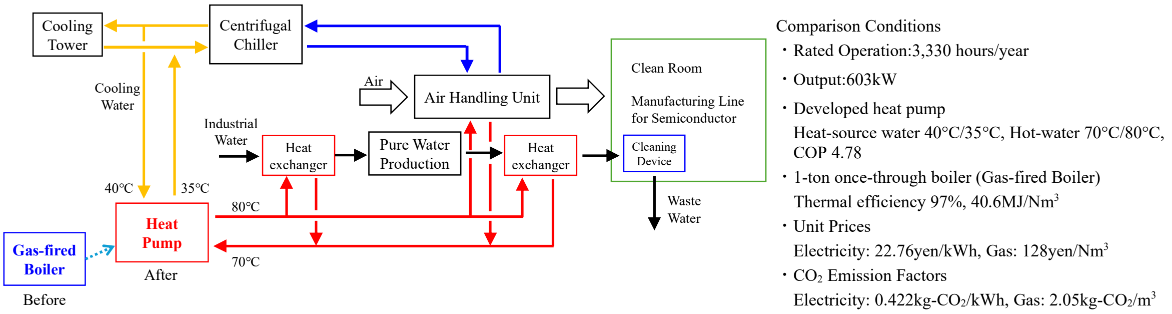

Figure 7. Application system

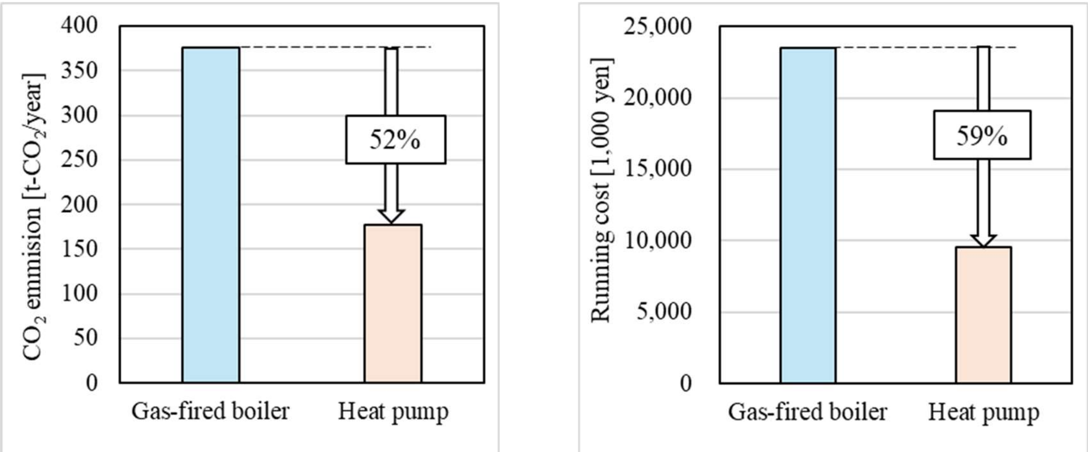

Figure 8. Reduction effects of using the heat pump on (left) CO_2 emissions and (right) running costs of the system shown in Fig. 7

5. Conclusions

We developed a large-capacity centrifugal heat pump using refrigerant HFO-1233zd(E) with a GWP of 1. The heat pump is designed to supply hot water up to 90°C for industrial applications. When validated in an actual machine, the maximum heating capacity was 670 kW at the outlet of 90°C hot water, and the COP reached 3.94. We further confirmed that the developed heat pump can significantly reduce CO_2 emissions when applied as a substitute of boilers. In the future, we plan to further expand the capacity of the heat pump.

References

[1] United Nations Environment Programme (UNEP), Kigali Amendment to the Montreal Protocol on Substances that Deplete the Ozone Layer (2016).
[2] Intergovernmental Panel on Climate Change (IPCC), Fourth Assessment Report (AR4), (2007) https://www.ipcc.ch/assessment-report/ar4/ (2023)
[3] Intergovernmental Panel on Climate Change (IPCC), Fifth Assessment Report (AR5), (2014) https://www.ipcc.ch/assessment-report/ar5/ (2023)
[4] NIST Reference Fluid Thermodynamic and Transport Properties Database (REFPROP) Version 10.0
[5] Ryosuke Suemitsu, Naoya Miyoshi, Yasushi Hasegawa, Kazuki Wajima, Yoshinori Shirakata, Kenji Ueda, "Development of centrifugal chiller and heat pump using low GWP refrigerant" 12th IEA Heat Pump Conference (2017)